


Synthesis of Two-Photon Active Tricomponent Fluorescent Probe for Distinguishment of Biotin Receptor Positive and Negative Cells and Imaging 3D-Spheroid

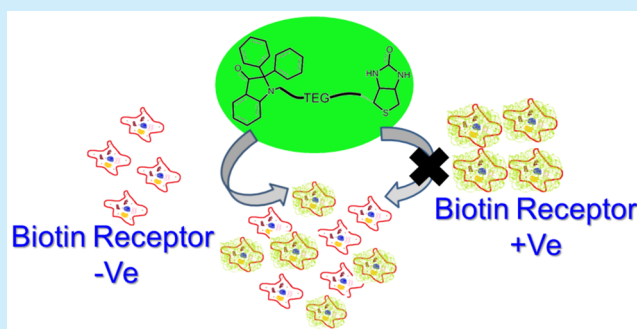
Kaushik Pal,[†] Aman Sharma,[‡] and Apurba L. Koner^{*,†} 

[†]Department of Chemistry, Indian Institute of Science Education and Research Bhopal, Bhopal Bypass Road, Bhauri, Bhopal-462066, India

[‡]ExoCan Healthcare Technologies Pvt. Ltd., Pune-411008, India

Supporting Information

ABSTRACT: A fluorescence microscopy-based distinguishment between biotin receptor (BiR) positive and negative cell lines *via* receptor-mediated endocytosis has been demonstrated. A water-soluble, three-component, two-photon (2P) active solvatofluorochromic probe has been designed and synthesized. The applicability of the probe for 2P microscopy and 3D-spheroid was also assessed.



For the development of specific therapeutics to combat cancer, cell-surface receptors (CSRs) are considered to be the most important targets.^{1–4} These CSRs are overexpressed in most of the cancer cells as compared to normal cells.^{4–7} Folate,⁸ insulin-like growth factor,⁹ epidermal growth factor,^{10,11} G protein-coupled,⁵ and biotin receptors (BiR)¹² are prototype examples of CSRs which are popular targets for cancer theranostics.^{13,14} Recently, BiR has been recognized as one of the important targets for the diagnosis and treatment of cancer for having a strong and specific interaction with biotin.^{4,15–17} Therefore, the understanding of a receptor-mediated endocytosis pathway and identification of CSR positive cells is crucial and prerequisite before the administration of therapeutics. Among the malignancy identification techniques, computed tomography (CT) and magnetic resonance imaging (MRI) were successfully used in the medical field.^{18–21} Recently, fluorescence microscopy and spectroscopy have been gaining tremendous popularity for biomolecular sensing, trafficking, or tissue imaging because of the benefits of high sensitivity, spatiotemporal accuracy, and low cost.^{10,22,23} Organic dyes, inorganic semiconductor quantum dot (Qdot), conjugated polymer-based nanoparticle (Pdot), and metal nanoclusters have gained immense popularity for both *in vitro* and *in vivo* applications.^{22,24–27} Qdot and Pdots are shown to have superior photostability and brightness. However, they are associated with long-term toxicity and large size compared to the associated biomolecules.^{28,29} Recently, an intense strategic effort has been employed for the development of small-sized organic dyes with good water solubility, high quantum yield, photostability, and robustness to the solution composition.^{22,30}

Herein, we have successfully distinguished BiR positive (HeLa)³¹ and negative (HEK-293)³² cells with a rational design and synthesis of biotin appended, two-photon (2P) active, and water-soluble fluorophore **5** (Scheme 1). This particular probe contains a fluorescent propellerocin moiety,²² tetraethylene glycol (TEG) as a water-soluble flexible linker, and biotin as the specific anchor to BiR for the endocytosis. Utilizing UV–vis., steady-state, and time-resolved fluorescence spectroscopy, the robustness and suitability of the probe for *in vitro* and *in vivo* applications were extensively investigated. Further, both single photon and 2P fluorescence microscopy were employed for 2D cell lines and 3D spheroids for an efficient differentiation of BiR positive cells.³³

Synthesis of the tricomponent probe was initiated with a TEG linker, which was modified with propargyl bromide, and compound **2** was obtained. Then biotin, the substrate of BiR, was appended *via* a simple ester coupling to obtain **3**. Finally, to construct desired compound **5**, copper(I)-assisted alkyne–azide click chemistry was employed to tether compound **3** with fluorescent propellerocin (Scheme 1 and Supporting Information). Compound **4** was synthesized using a reported protocol.²² Over the years, quite a few biotin-conjugated fluorophores were developed for BiR targeting applications; however, compound **5** has several advantages over them as shown in Table S1.

It is observed quite often that synthetic modification especially with a flexible linker may affect the photophysical

Received: August 27, 2018

Scheme 1. Synthesis of Three-Component 2P Active Fluorophore 5

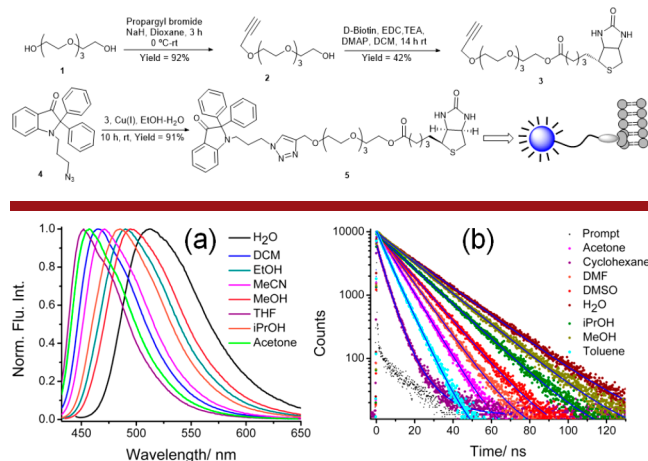


Figure 1. Solvatochromic behavior of **5**. (a) Solvent polarity-dependent normalized fluorescence spectra and (b) fluorescence lifetime decay profile.

Table 1. Solvent-Dependent Optical Properties of 5

solvent	$\lambda_{\text{abs}}^{\text{max}}$ (nm)	$\lambda_{\text{flu}}^{\text{max}}$ (nm)	$QY^{a,b}$	τ (ns) ^b
H ₂ O	435	512	0.57	19.6
ethylene glycol	428	500	0.71	19.5
MeOH	425	495	0.58	17.8
EtOH	423	490	0.54	16.6
<i>i</i> -PrOH	421	485	0.56	15.6
MeCN	421	470	0.38	11.9
DMSO	426	469	0.50	12.5
CHCl ₃	420	468	0.48	10.9
EtOAc	423	467	0.30	9.7
DCM	422	465	0.45	10.6
DMF	422	463	0.37	10.5
acetone	425	460	0.32	8.6
benzene	416	458	0.28	6.8
toluene	415	455	0.25	6.5
THF	418	452	0.24	6.4

^aMeasured with respect to 1,8-ANS in methanol.³⁴ ^b5% error in measurements.

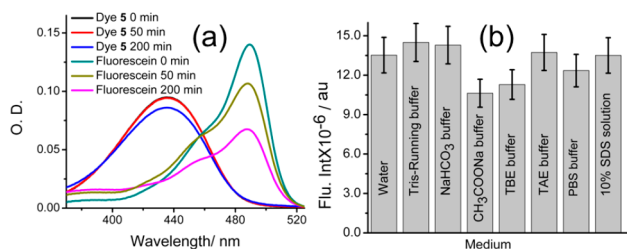


Figure 2. High photostability and robust fluorescence properties of **5** in different buffer. (a) Absorption spectra of **5** and fluorescein are plotted after illumination under white light under identical conditions; (b) fluorescence intensity of **5** in various commonly used buffers.

properties of the core fluorophore. Therefore, we wanted to verify if there is any such undesired properties present or not. The UV-vis. investigations show that the ground-state behavior of **5** is hardly affected by the environmental polarity (Figure S1, Table 1). However, in water, **5** has an emission maximum at 512 nm whereas it shows a blue-shifted peak at

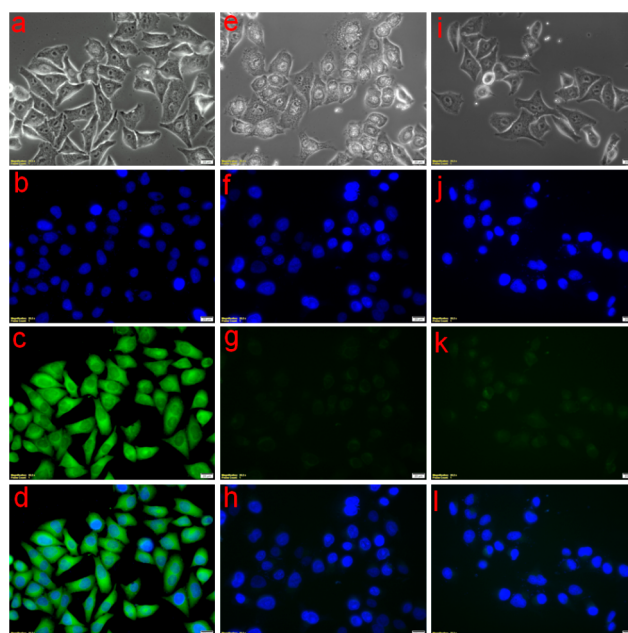


Figure 3. Live-cell fluorescence imaging of BiR positive cell under (HeLa) free-ligand competition and metabolism-block conditions. (a–d) Cells were incubated with 5 μM probe for 1 h, and images were acquired using phase contrast mode, blue channel (350/470 excitation/emission filter cube, nucleus stain Hoechst-33342), green channel (490/525 excitation/emission filter cube for **5**), and merge. (e–h) Cells were treated with 1 mM of D-biotin for 1 h prior incubation with **5**. (i–l) Cells were treated with 0.05% (w/v) NaN_3 for 0.5 h prior to incubation with identical concentration (image acquired: a, e, and i phase contrast; b, f, and j blue channel; c, g, and k green channel; and d, h, and l are merge of blue and green channel).

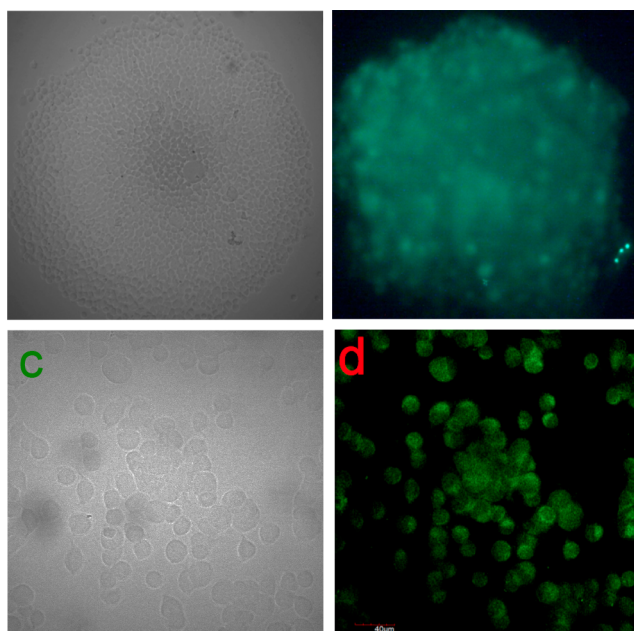


Figure 4. Imaging in 3D spheroid and using 2P fluorescence microscopy. (a–b) 3D spheroid derived from HUVEC cells was incubated with 10 μM of **5** and imaged under fluorescence microscope and (c–d) live-cell fluorescence imaging under 2P (820 nm laser) excitation using HeLa cells: incubated with **5** (5 μM) and emission collected in the range of 450–550 nm (scale 40 μm).

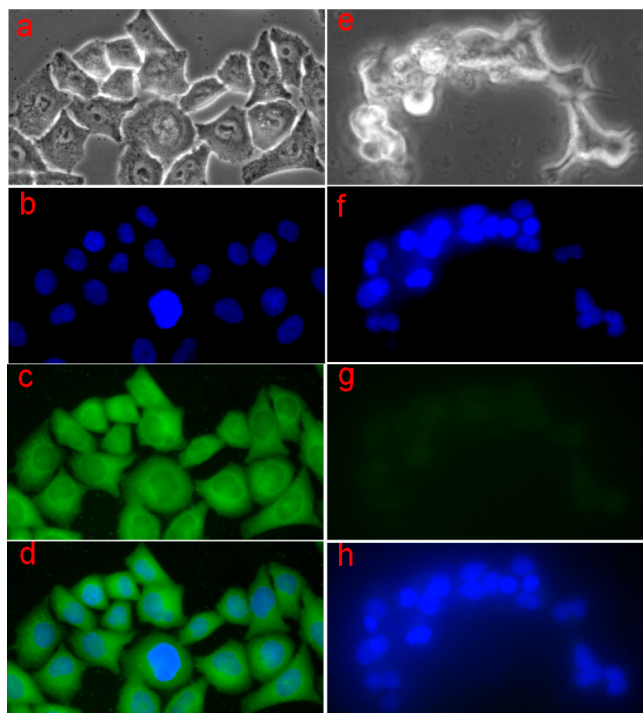


Figure 5. Differentiation between BiR positive (HeLa) and negative (HEK-293) cell lines *via* live-cell fluorescence imaging. (a–d) HeLa cells were incubated with **5** for 1 h; shown are images acquired in phase contrast, blue channel (350/470 excitation/emission filter cube), green channel (490/525 excitation/emission filter cube), and merge of blue and green channel, respectively. (e–h) HEK-293 cells were incubated with **5**; image sequence same as that used previously (image acquired: a and e, phase contrast; b and f, blue channel; c and g, green channel; and d and h are merge of blue and green channel).

452 nm in less polar solvent such as THF (Figure 1a, Table 1). A linear correlation between the emission maxima and the solvent polarity parameter $E_T(30)$ implies that the probe exhibits no specific solvent effect. On the other hand, the results from the fluorescence lifetime experiment also show considerable solvent polarity dependence. The excited-state lifetime became longer (Figure 1b) with the increase in solvent polarity. The longer lifetime together with the high quantum yield offers the possibility of fluorescence lifetime-based imaging.

To visualize the biomolecular dynamics in live cells, fluorescence microscopy is one of the most popular and widely used techniques. However, photobleaching due to exposure to light is known to affect the brightness and long-term fluorescence imaging.^{35,36} To investigate the photostability of **5**, a comparative photostability experiment was performed with widely used microscopy dye fluorescein (with comparable photophysics) which revealed that **5** is far more photochemically stable than that of fluorescein. The photostability experiment was performed in PBS illuminated with a visible lamp equipped with a photoreactor where the light intensity was 12 000 lx. After 200 min of exposure to visible light, fluorescein loses more than 50% of its absorbance whereas **5** loses only up to 10% (Figure 2a). Furthermore, fluoroprobe **5** showed remarkable thermostability up to 50 °C (Figure S2) and pH stability over a wide range (Figure S3). We have also monitored the fluorescence intensity of **5** in a wide range of biologically relevant buffers and 10% SDS

solution and only observed minimal change in the fluorescence intensity (Figure 2b).

After a detailed investigation of photophysical properties, we have assayed the BiR mediated endocytosis and cellular internalization process. In this regard, we have chosen BiR positive cell line HeLa as the positive control¹⁴ and subjected it to various conditions (Figure 3). In condition I, cells were incubated with 5 μ M of **5** and 1 μ M of Hoechst-33342 (blue fluorescence, nucleus-specific dye) for 1 h and imaged under a microscope; the results are shown in Figure 3a–d. In this case, cells showed very bright fluorescence intensity (imaged in the green channel) due to **5**, which indicated efficient cellular internalization. However, in condition II, cells were pretreated with 1 mM of D-biotin (substrate for BiR) for 1 h before applying condition I. Indeed, the results shown in Figure 3e–h clearly indicate that the cellular intake was mediated by BiR, as the fluorescence intensity in the green channel corresponding to **5** was very weak. The blocking of BiR is responsible for the low level of cellular uptake of **5**. To reconfirm the endocytosis process, which is responsible for the cellular internalization, we have utilized metabolism inhibitor NaN₃ in condition III. Similar to the biotin-block condition, the feeble fluorescence originated due to the negligible amount of endocytosis of **5** (Figure 3i–l).

Conventionally, one-photon fluorescence microscopy is carried out with a monolayer of cells, spread over a 2D surface, which does not provide geometrical, mechanical, and biochemical comparability with the real tissues. The outcome of those *in vitro* studies face thoughtful criticism due to lack of accuracy when similar experiments were conducted with the real biological tissues.^{33,37} Therefore, to overcome such issues, researchers have attempted using 3D cell culture for shrinking the gap between real tissues and *in vitro* models.³⁷ 3D cell culture models proved to be closer to the real *in vivo* model. On this basis, we have tested our synthesized probe in 3D spheroids and observed a comprehensive cellular uptake (Figure 4a–b).

Another major problem associated with deep tissue imaging is the penetration of the excitation light and autofluorescence. To overcome these problems, the design of 2P active fluorescent probes was carried out.³⁸ The present probe contains an ICT moiety, and generally, the molecules containing an electron donor and acceptor groups are established as 2P active.^{39,40} To validate further the applicability of **5** for deep tissue fluorescence imaging, we have performed 2P microscopy using an IR laser (820 nm) as the excitation source. As per our expectation, we obtained a strong 2P fluorescence signal with a low autofluorescence background as shown in Figure 4c–d. After confirming the BiR mediated endocytosis-based cellular internalization of **5** and potentiality for use as a 2P active probe and applicability in 3D spheroids, we extended our study toward differentiation of BiR positive and negative cells. HeLa cells are known for the overexpression of BiR while HEK-293 expresses an alleviated amount compared to HeLa.¹⁴ We have cultured and incubated them in aforementioned conditions and performed fluorescence microscopy. Indeed, HeLa cells showed much brighter fluorescence as compared to HEK-293 due to better cellular intake assisted by overexpressed BiR (Figure 5). This confirms the differentiation between BiR positive and negative cells *via* fluorescence microscopy.

In conclusion, we have successfully designed and synthesized an indoline-based D-biotin-conjugated, 2P active, three-

component, and water-soluble fluorescent dye, with strong solvatochromism. The potentiality of the probe has been comprehensively proven by its high fluorescence quantum yield, photostability, thermostability, and retention of fluorescence intensity in a wide variety of buffer solutions. After confirming BiR mediated endocytosis, we successfully employed this molecule to differentiate between BiR positive (HeLa) and negative (HEK-293) cells. The applicability of the probe was also investigated with 3D spheroid and 2P microscopy. We firmly believe that this presented strategy with an environment-sensitive small organic dye will be highly important for pretherapeutic diagnosis.

■ ASSOCIATED CONTENT

● Supporting Information

The Supporting Information is available free of charge on the ACS Publications website at DOI: [10.1021/acs.orglett.8b02748](https://doi.org/10.1021/acs.orglett.8b02748).

Details of synthesis and cell-culture protocol, characterization by NMR, mass spectrometry and UV-vis spectroscopy (PDF)

■ AUTHOR INFORMATION

Corresponding Author

*E-mail: akoner@iiserb.ac.in

ORCID 

Apurba L. Koner: [0000-0002-8891-416X](https://orcid.org/0000-0002-8891-416X)

Notes

The authors declare no competing financial interest.

■ ACKNOWLEDGMENTS

We acknowledge the financial support from Department of Biotechnology (DBT, BT/PR14498/NNT/28/880/2015), India. K.P. gratefully acknowledges CSIR, India for his doctoral fellowship. We acknowledge sophisticated instrumentation facility IIT Indore for the two-photon imaging. We thank Mr. Rupam Roy for his help with NMR measurements.

■ REFERENCES

- (1) Lv, L.; Liu, C. X.; Chen, C. X.; Yu, X. X.; Chen, G. H.; Shi, Y. H.; Qin, F. C.; Ou, J. B.; Qiu, K. F.; Li, G. C. Quercetin and doxorubicin co-encapsulated biotin receptor-targeting nanoparticles for minimizing drug resistance in breast cancer. *Oncotarget* **2016**, *7*, 32184–32199.
- (2) Heo, D. N.; Yang, D. H.; Moon, H. J.; Lee, J. B.; Bae, M. S.; Lee, S. C.; Lee, W. J.; Sun, I. C.; Kwon, I. K. Gold nanoparticles surface-functionalized with paclitaxel drug and biotin receptor as theranostic agents for cancer therapy. *Biomaterials* **2012**, *33*, 856–866.
- (3) Qu, W.; Ren, S.; Kuang, Y.; Jiang, X. J.; Zhuo, R. X.; Zhang, X. Z. Mimicking the Biological Ligand-Receptor Principle for Universal Target Gene Delivery Mediated by Avidin-Biotin Interaction. *Adv. Healthcare Mater.* **2013**, *2*, 418–421.
- (4) Ren, W. X.; Han, J. Y.; Uhm, S.; Jang, Y. J.; Kang, C.; Kim, J. H.; Kim, J. S. Recent development of biotin conjugation in biological imaging, sensing, and target delivery. *Chem. Commun.* **2015**, *51*, 10403–10418.
- (5) Dorsam, R. T.; Gutkind, J. S. G-protein-coupled receptors and cancer. *Nat. Rev. Cancer* **2007**, *7*, 79–94.
- (6) Russell-Jones, G.; McTavish, K.; McEwan, J.; Rice, J.; Nowotnik, D. Vitamin-mediated targeting as a potential mechanism to increase drug uptake by tumours. *J. Inorg. Biochem.* **2004**, *98*, 1625–1633.
- (7) Pal, K.; Heinsch, A.; Berkessel, A.; Koner, A. L. Differentiation of Folate-Receptor-Positive and -Negative Cells Using a Substrate-Mimicking Fluorescent Probe. *Chem. - Eur. J.* **2017**, *23*, 15008–15011.
- (8) Parker, N.; Turk, M. J.; Westrick, E.; Lewis, J. D.; Low, P. S.; Leamon, C. P. Folate receptor expression in carcinomas and normal tissues determined by a quantitative radioligand binding assay. *Anal. Biochem.* **2005**, *338*, 284–293.
- (9) Boone, D. N.; Lee, A. V. Targeting the Insulin-like Growth Factor Receptor: Developing Biomarkers from Gene Expression Profiling. *Crit. Rev. Oncog.* **2012**, *17*, 161–173.
- (10) Gao, M.; Su, H.; Lin, G.; Li, S.; Yu, X.; Qin, A.; Zhao, Z.; Zhang, Z.; Tang, B. Z. Targeted imaging of EGFR overexpressed cancer cells by brightly fluorescent nanoparticles conjugated with cetuximab. *Nanoscale* **2016**, *8*, 15027–15032.
- (11) Jung, K. H.; Park, J. W.; Paik, J. Y.; Quach, C. H. T.; Choe, Y. S.; Lee, K. H. EGF receptor targeted tumor imaging with biotin-PEG-EGF linked to Tc-99m-HYNIC labeled avidin and streptavidin. *Nucl. Med. Biol.* **2012**, *39*, 1122–1127.
- (12) Niers, J. M.; Chen, J. W.; Weissleder, R.; Tannous, B. A. Enhanced in Vivo Imaging of Metabolically Biotinylated Cell Surface Reporters. *Anal. Chem.* **2011**, *83*, 994–999.
- (13) Bhuniya, S.; Maiti, S.; Kim, E.-J.; Lee, H.; Sessler, J. L.; Hong, K. S.; Kim, J. S. An Activatable Theranostic for Targeted Cancer Therapy and Imaging. *Angew. Chem., Int. Ed.* **2014**, *53*, 4469–4474.
- (14) Ren, W. X.; Han, J.; Uhm, S.; Jang, Y. J.; Kang, C.; Kim, J.-H.; Kim, J. S. Recent development of biotin conjugation in biological imaging, sensing, and target delivery. *Chem. Commun.* **2015**, *51*, 10403–10418.
- (15) Xia, C. F.; Zhang, Y.; Zhang, Y.; Boado, R. J.; Pardridge, W. M. Intravenous siRNA of brain cancer with receptor targeting and avidin-biotin technology. *Pharm. Res.* **2007**, *24*, 2309–2316.
- (16) Sun, Q.; Sun, D.; Song, L.; Chen, Z.; Chen, Z.; Zhang, W.; Qian, J. Highly Selective Fluorescent Turn-On Probe for Protein Thiols in Biotin Receptor-Positive Cancer Cells. *Anal. Chem.* **2016**, *88*, 3400–3405.
- (17) Shin, W. S.; Han, J.; Kumar, R.; Lee, G. G.; Sessler, J. L.; Kim, J.-H.; Kim, J. S. Programmed activation of cancer cell apoptosis: A tumor-targeted phototherapeutic topoisomerase I inhibitor. *Sci. Rep.* **2016**, *6*, 29018.
- (18) Edelman, R. R.; Warach, S. Magnetic Resonance Imaging. *N. Engl. J. Med.* **1993**, *328*, 708–716.
- (19) Gambhir, S. S. Molecular imaging of cancer with positron emission tomography. *Nat. Rev. Cancer* **2002**, *2*, 683–693.
- (20) Kong, X.; Dong, B.; Zhang, N.; Wang, C.; Song, X.; Lin, W. A unique red-emitting two-photon fluorescent probe with tumor-specificity for imaging in living cells and tissues. *Talanta* **2017**, *174*, 357–364.
- (21) Jang, J. H.; Kim, W. R.; Sharma, A.; Cho, S. H.; James, T. D.; Kang, C.; Kim, J. S. Targeted tumor detection: guidelines for developing biotinylated diagnostics. *Chem. Commun.* **2017**, *53*, 2154–2157.
- (22) Pal, K.; Koner, A. L. Rationally Designed Solvatochromic Fluorescent Indoline Derivatives for Probing Mitochondrial Environment. *Chem. - Eur. J.* **2017**, *23*, 8610–8614.
- (23) Yuan, L.; Lin, W.; Zheng, K.; He, L.; Huang, W. Far-red to near infrared analyte-responsive fluorescent probes based on organic fluorophore platforms for fluorescence imaging. *Chem. Soc. Rev.* **2013**, *42*, 622–661.
- (24) Koner, A. L.; Krndija, D.; Hou, Q.; Sherratt, D. J.; Howarth, M. Hydroxy-Terminated Conjugated Polymer Nanoparticles Have Near-Unity Bright Fraction and Reveal Cholesterol-Dependence of IGF1R Nanodomains. *ACS Nano* **2013**, *7*, 1137–1144.
- (25) Chen, J.; Chen, Q.; Gao, C.; Zhang, M.; Qin, B.; Qiu, H. A SiO₂ NP-DNA/silver nanocluster sandwich structure-enhanced fluorescence polarization biosensor for amplified detection of hepatitis B virus DNA. *J. Mater. Chem. B* **2015**, *3*, 964–967.

- (26) Kim, G.-J.; Lee, K.; Kwon, H.; Kim, H.-J. Ratiometric Fluorescence Imaging of Cellular Glutathione. *Org. Lett.* **2011**, *13*, 2799–2801.
- (27) Liu, T.; Xu, Z.; Spring, D. R.; Cui, J. A Lysosome-Targetable Fluorescent Probe for Imaging Hydrogen Sulfide in Living Cells. *Org. Lett.* **2013**, *15*, 2310–2313.
- (28) Hardman, R. A Toxicologic Review of Quantum Dots: Toxicity Depends on Physicochemical and Environmental Factors. *Environ. Health Perspect.* **2006**, *114*, 165–172.
- (29) Zhang, S.; Li, J.; Lykotrafitis, G.; Bao, G.; Suresh, S. Size-Dependent Endocytosis of Nanoparticles. *Adv. Mater.* **2009**, *21*, 419–424.
- (30) Kowada, T.; Maeda, H.; Kikuchi, K. BODIPY-based probes for the fluorescence imaging of biomolecules in living cells. *Chem. Soc. Rev.* **2015**, *44*, 4953–4972.
- (31) Yuan, Z.; Zhao, D.; Yi, X.; Zhuo, R.; Li, F. Steric Protected and Illumination-Activated Tumor Targeting Accessory for Endowing Drug-Delivery Systems with Tumor Selectivity. *Adv. Funct. Mater.* **2014**, *24*, 1799–1807.
- (32) Brahmachari, S.; Ghosh, M.; Dutta, S.; Das, P. K. Biotinylated amphiphile-single walled carbon nanotube conjugate for target-specific delivery to cancer cells. *J. Mater. Chem. B* **2014**, *2*, 1160–1173.
- (33) Zanoni, M.; Piccinini, F.; Arienti, C.; Zamagni, A.; Santi, S.; Polico, R.; Bevilacqua, A.; Tesei, A. 3D tumor spheroid models for in vitro therapeutic screening: a systematic approach to enhance the biological relevance of data obtained. *Sci. Rep.* **2016**, *6*, 19103.
- (34) Kosower, E. M.; Kanety, H. Intramolecular donor-acceptor systems. 10. Multiple fluorescences from 8-(N-phenylamino)-1-naphthalenesulfonates. *J. Am. Chem. Soc.* **1983**, *105*, 6236–6243.
- (35) Yao, J.; Yang, M.; Duan, Y. Chemistry, Biology, and Medicine of Fluorescent Nanomaterials and Related Systems: New Insights into Biosensing, Bioimaging, Genomics, Diagnostics, and Therapy. *Chem. Rev.* **2014**, *114*, 6130–6178.
- (36) Marx, V. Probes: paths to photostability. *Nat. Methods* **2015**, *12*, 187–190.
- (37) Pampaloni, F.; Ansari, N.; Stelzer, E. H. K. High-resolution deep imaging of live cellular spheroids with light-sheet-based fluorescence microscopy. *Cell Tissue Res.* **2013**, *352*, 161–177.
- (38) Theer, P.; Hasan, M. T.; Denk, W. Two-photon imaging to a depth of 1000 μm in living brains by use of a Ti:Al₂O₃ regenerative amplifier. *Opt. Lett.* **2003**, *28*, 1022–1024.
- (39) Helmchen, F.; Denk, W. Deep tissue two-photon microscopy. *Nat. Methods* **2005**, *2*, 932.
- (40) Pal, K.; Samanta, I.; Gupta, R. K.; Goswami, D.; Koner, A. L. Deciphering micro-polarity inside the endoplasmic reticulum using a two-photon active solvatofluorochromic probe. *Chem. Commun.* **2018**, *54*, 10590–10593.